

We are IntechOpen, the world's leading publisher of Open Access books Built by scientists, for scientists

6,900

Open access books available

186,000

International authors and editors

200M

Downloads

Our authors are among the

154

Countries delivered to

TOP 1%

most cited scientists

12.2%

Contributors from top 500 universities



WEB OF SCIENCE™

Selection of our books indexed in the Book Citation Index
in Web of Science™ Core Collection (BKCI)

Interested in publishing with us?
Contact book.department@intechopen.com

Numbers displayed above are based on latest data collected.
For more information visit www.intechopen.com



Hyperspectral Data Analysis and Visualisation

Maarten A. Hogervorst and Piet B.W. Schwering
*TNO Defense & Security,
The Netherlands*

1. Introduction

Electro-Optical (EO) imaging sensors are widely used for a range of tasks, e.g. for Target Acquisition (TA: detection, recognition and identification of (military) relevant objects) or visual search. These tasks can be performed by a human observer, by an algorithm (Automatic Target Recognition) or by both (Aided Target Recognition). In the past decades, the development of night vision devices in the thermal infrared and image intensifying systems has greatly extended the applicability of EO systems. Despite of these rapid developments, the current generation of sensors has important limitations. Until now, operational thermal imagers are sensitive to IR (infrared) radiation from a single spectral band in the Long Wave (8-14 μm , LWIR) or Mid Wave (3-5 μm , MWIR) infrared region. These so-called broad band sensors basically produce a monochrome (i.e. a black-and-white pan-chromatic) image that deviates considerably from a normal daylight view, and is based on temperature contrasts in a scene. With these systems, the distinction between real targets and decoys, or between military and civilian targets is often difficult to make. Also, camouflaged targets or targets that are hidden deep in the woods are difficult to detect. Recognizing different objects and materials may be difficult. Examples of misinterpretations when using an Image Intensifier system are grass that looks like snow, or trees that look like bushes, when seen from a helicopter. These misinterpretations may lead to disorientation (loss of Situational Awareness) or to a (fatal) wrong distance estimation.

Currently, multi-band and hyperspectral imaging sensors in the thermal infrared are under development. Traditionally hyperspectral imagers were developed for satellites with applications ranging from monitoring the environment, climate analysis, detection of pollution and fires. These systems also promise significant improvements in military task performance. With these new systems, targets may be distinguished not only on the basis of differences in radiation magnitude, but also on differences in spectral properties. Multi-band sensors are sensitive to several (2 to 10) sub-bands in a spectral region. Hyperspectral sensors are sensitive to many (in the order of 100) sub-bands. Hyperspectral sensors have existed for a while, and have mainly been used for remote sensing from an airborne platform or a satellite. Only recently these sensors entered the infrared spectral sensitivity regions. A recent overview on hyper spectral image technology is provided by Vagni (1990). Present-day hyperspectral sensors typically contain a very high number of spectral bands. The penalty for using such a high number of spectral bands is that for each spectral-band image the averaged signal-to-noise ratio is smaller than for a broad band sensor. Operational hyperspectral systems will be complex and expensive because of the wavelength discrimination element in the sensor. This is especially true for the infrared wavelength

range. Furthermore, the processing of this huge amount of data of a hyperspectral image cube may be troublesome. It complicates a near real-time image processing solution for automatic target detection. Band selection is therefore seen as an important step in realizing effective operational hyper/multi-spectral imaging solutions.

Hyperspectral sensors provide a large amount of information (a three-dimensional, 3-D, hypercube with the 3rd dimension coding the spectral information) at the cost of a reduced speed. The additional spectral information from multi-band or hyperspectral sensors may be used, for instance, for *automatic detection*, recognition or identification. Alternatively, the information is visualised for *human inspection*. In addition, alternative presentation methods to human observers are possible. Ergonomic presentation techniques may simplify the interpretation of the images and enhance performance, situational awareness and/or viewing comfort. Until now, the potential of the new systems is largely unknown and it is not clear how the 3-D hypercube data should be presented to the observers. Human and automatic target acquisition both have their advantages and disadvantages. In this study we focus on human target acquisition performance, although this may be supported by automatically derived information. Automatic detection processes could support the operator in a tedious task of scanning through large amounts of data, while the operator can spend his time to classifying automatically detected objects. A major advantage of the human visual system (HVS) is its superiority in pattern recognition. It is able to analyze an image at different (spatial and temporal) scales simultaneously and the interpretation is robust to spatial and temporal noise and to many types of image distortions. Humans are very flexible and able to tell which part of an image differs from the background without the need to specify what characterizes these differences. In contrast to automatic target recognition systems the number of assumptions (about signature of target and background, target shape etc.) can be small. We argue that often the final interpretation is best left to a human observer. Of course, when more knowledge about target and background (signature, shape etc.) is available this can be used to help the observer interpreting the data. A combination of automatic target recognition and presentation techniques (i.e. aided target recognition) can elevate the drawbacks of the use of human interpreters, such as limited processing capacity, processing time, memory and attention. A problem with presenting hyperspectral imagery to a human observer is the huge amount of information. The question is how the data should be made available to the human visual system, i.e. which presentation offers sufficient, or the best, information transfer. This also depends on the task at hand (e.g. detection, situational awareness, identification) and the prior information available. Several applications are available that support the processing and analysis of hyperspectral data (e.g. MicroMSI, Opticks, Envi). The emphasis in these applications lies on the processing algorithms. Here, we focus on the development and evaluation of presentation methods that optimize the information transfer to the human operator.

2. Optimal band selection

Most research involving band selection has focussed only on small bands of single or a few wavelengths. However, for a multispectral configuration narrow bands are not practical, due to the limited signal-to-noise ratio, and this would require long integration times to get a good signal-to-noise ratio. Our research therefore not only looks at the location of the bands but also at the width of the bands. In our previous research (Withagen et al., 2001) a first attempt was made by developing an algorithm that first determines the best locations,

in terms of maximizing information content in a limited set of wavelengths, for the bands and than the best width of the bands. This however does not allow for a comparison between broad and narrow bands. Therefore a new algorithm has been written to find the set of bands with optimal information, given the number of bands and their width.

2.1 Band selection method

We have developed two versions of the algorithm, a fast one that can quickly find a solution but does not guarantee to find the best bands, and an optimal algorithm, which searches all possible combinations but as a consequence takes a lot longer and can only be used if the number of required bands is small. In this way information content is optimized under the set boundary conditions. Each band combination is evaluated a distance measure that quantifies the separation between classes. We use two different distance measures (Landgrebe, 2003). The Mahalanobis distance and the Bhattacharyya distance, which are both described below.

The Mahalanobis distance is defined as:

$$D = \sqrt{[\mu_1 - \mu_2] \Sigma^{-1} [\mu_1 - \mu_2]^T} \quad (1)$$

Where μ_1 and μ_2 are the class averages of the target class (class 1) and background class (class 2) and Σ is the covariance matrix of these classes.

When using the Mahalanobis distance measure one has to keep in mind that the following assumptions are made:

- The distributions of the classes are multivariate Gaussian distributions.
- The covariance matrix of these distributions is the same for all classes.
- The total number of pixels is large enough to accurately describe the covariance matrix (a rule of thumb is that the number of pixels should be at least 10 times the number of dimensions).

The distance measure is implemented by first transforming the feature-space and then calculating the Euclidian distance between the centres of the classes in this transformed feature space. The transformation makes use of the average covariance matrix of the different classes involved. The data is transformed to a different feature-space by multiplying it with the eigenvectors of this covariance matrix. The effect of this transformation is that the data is de-correlated.

The advantage of this transformation is visible in Figure 1. In the original feature-space (Figure 1a) the distance between background class BG1 (in light green) and background class BG2 (in dark green) is larger than the distance between background class BG1 (light green) and target class T1 (red), and hence the separability between classes BG1 and BG2 is better. In the transformed feature-space (Figure 1b) the classes which are most easy to separate also have the highest Euclidian distance. In the transformed feature-space the Euclidian distance is calculated between the centres of the different classes. The resulting set of distances is then stored in a distance matrix. From this matrix a final single distance value is derived in several ways depending on the experimental requirements (for example the minimum value of this matrix can be taken). Because we want to distinguish between background and target classes we choose the smallest distance between a target and a background class. This final distance value we will refer to as the quality of a band combination. In the band selection algorithm this quality is maximized.

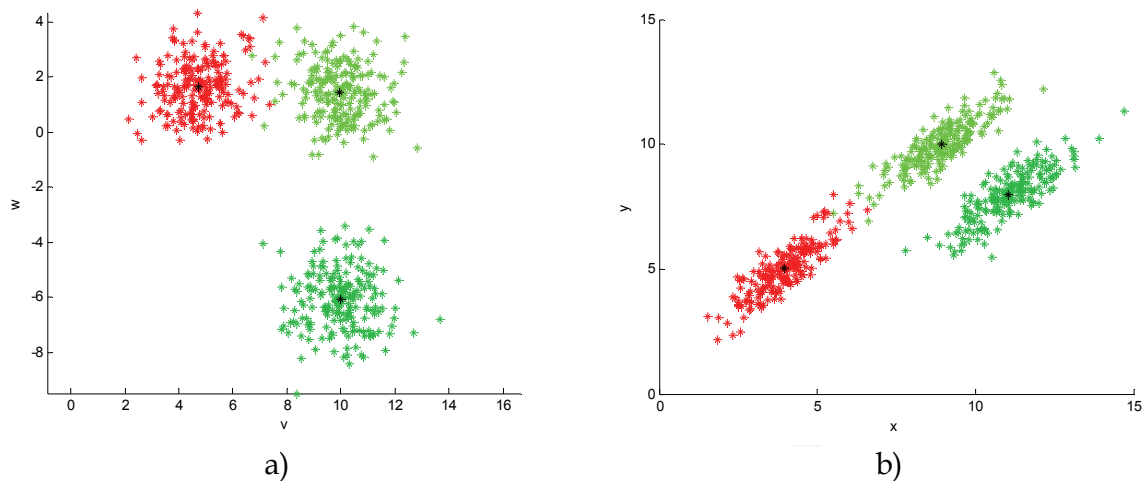


Fig. 1. Example of a 2D feature-space (a) and its transformation (b).

The Bhattacharyya distance is another distance measure that measures the distance between two multivariate Gaussian distributions. It is defined as:

$$B = \frac{1}{8} [\mu_1 - \mu_2]^T \left[\frac{\Sigma_1 + \Sigma_2}{2} \right]^{-1} [\mu_1 - \mu_2] + \frac{1}{2} \ln \frac{|1/2[\Sigma_1 + \Sigma_2]|}{\sqrt{|\Sigma_1||\Sigma_2|}} \quad (2)$$

One important difference with the Mahalanobis distance is that it does not take the average covariance matrix of the classes but keeps the class covariance matrices. The price that has to be paid in this case is that now each class has to contain enough pixels to describe its covariance matrix accurately.

2.2 Optimization of band selection

In order to find the best band combination two algorithms have been developed. The first algorithm searches all possible band combinations. This algorithm can only be used if the number of required bands is small (<4) because the calculation time increases exponentially with the number of bands. Therefore a second algorithm has been developed that searches in a more time efficient way, but as a consequence it is not guaranteed to find the optimum band combination.

The algorithms are implemented in Matlab® and make use of the toolbox PRTools, a toolbox offered for free for academic research by the University of Delft in The Netherlands. The main data-object of PRTools is called the dataset. In this dataset a large number of objects can be stored, each object consisting of a certain amount of features. We use this dataset-type to store our pixel-data. The dataset-object also makes it possible to label each object with an integer value, which can be used to divide the pixels in different classes.

We have analyzed the effects of the two algorithms:

- Algorithm 1 is the fast algorithm. The way it selects its bands is by first selecting the band with the highest quality. Then it searches for a second band that, combined with the already found band, gives the highest quality. Then it searches for a third band in the same way and this process continues way until the required number of bands are found.
- Algorithm 2 (called the optimum algorithm) searches every possible combination of bands, which guarantees that it will find the band combination with the highest quality. Because calculation times increase exponentially with the number of bands, it can only be used if the number of bands required is small. The algorithm can also be used in a sub-

optimal way, by defining a step-parameter (see below) higher than 1, in which case the algorithm gets faster. Besides a potentially better solution, Algorithm 2 has another advantage with respect to Algorithm 1: because it calculates the quality for each combination, an overview of all qualities can be made, giving extra insight in the problem. To perform classification, the quadratic discriminant classifier (QDC) provided by PRTools is used. This is a quadratic classifier based on normal densities. For the two algorithms several inputs are needed:

- number of background classes,
- bandwidth,
- shape,
- distance type,
- overlap,
- quality criteria.

For Algorithm 2 we also set a step and time estimation parameter. For TimeEstimation, if 1, the algorithm makes an estimate of the calculation time by calculating how many combinations it will have to evaluate and multiplying this with the quality evaluation-time, which it gets by making 5 evaluations and taking the average. A Step parameter (default is 1) is defined to use the algorithm in a faster, sub-optimal way. The idea behind this parameter is that when for example a bandwidth of 30 features is used, the band consisting of features 1 through 30 will almost be exactly the same as band 2-31. By setting a step of for example 3, the algorithm will only take into account bands 1-30, 4-33, 7-36 and so on, which can greatly decrease the calculation-time without sacrificing much of the optimality of the solution.

If the overlap parameter is set to 0 (no overlap allowed), the bandwidth has also some influence on the calculation time. The larger the bandwidth the faster the algorithm will be because after the first band has been picked all features that make up this band are excluded for the following bands so effectively the total number of features decreases. Table 1 shows the calculation times of the Matlab implementation of Algorithm 1 for several numbers of bands using the Bhattacharyya or the Mahalanobis distance. The bandwidth used is 1. The number of pixels used is 1000. From this table we can conclude that the calculation of the Bhattacharyya distance takes on average about 30% less time than the calculation of the Mahalanobis distance.

number of bands	calculation time Bhattacharyya [s]	calculation time Mahalanobis [s]
2	8.5	16.0
4	19.0	31.9
6	30.9	47.7
8	43.5	63.7
10	57.3	80.3

Table 1. Band-selection calculation times for Algorithm 1 (the fast algorithm), with $\text{max_overlap} = 0$ and $\text{band_width} = 1$. The number of pixels used is 1000. Obviously calculation times are hardware dependent, but the important factor is the relative speed of the various runs.

Calculation times for Algorithm 2 are substantially longer than those of Algorithm 1. The relation between the calculation time, the number of bands and the total number of features for this algorithm is:

$$calc_time \sim no_pixels \cdot \frac{total_features!}{no_bands!(total_features - no_bands)!} \quad (3)$$

Depending on the value of the max_overlap parameter, the bandwidth also has a large influence on the calculation time. In Table 2 some calculation times are given for three different bandwidths and two different numbers of bands. max_overlap is set at 0 and the distance measure is Bhattacharyya. The Mahalanobis distance measure shows the same pattern but the calculation times are about 30% higher.

number of bands	Step: 1			Step: 2		
	1	10	30	1	10	30
2	00:10:03	00:07:20	00:04:58	00:02:10	00:01:50	00:00:54
3	10:33:20	07:30:00	02:08:20	01:13:20	00:48:57	00:16:10

Table 2. Band selection calculation times (hh:mm:ss) for Algorithm 2, using the Bhattacharyya distance measure, with max_overlap = 0 and band_width = 1, 10 and 30. The number of pixels used is 1000. For step parameter = 1, 2.

2.3 Results of band selection

To analyze the speed of the fast Algorithm 1 compared to slow, but optimal, Algorithm 2 a comparison has been made for a representative data set for the case that several targets are used with the following input settings:

- bandwidth = 30
- number of bands = 3
- step = 2
- overlap = 0

The data that was used consists of camouflaged military vehicles in a rural environment. Figure 3 shows an example of a typical image.

The comparison has been made for the Bhattacharyya as well as the Mahalanobis distance. Table 3 summarizes the result.

	Algorithm 1 bhattacharyya	Algorithm 2 bhattacharyya	Algorithm 1 mahalonobis	Algorithm 2 mahalonobis
Quality	0.4745	0.5450	2.3396	2.7131
QDC class. Error (miss-classified pixels)	75	76	81	78
band 1 (#features)	80 - 109	81 - 110	6 - 35	7 - 36
band 2 (#features)	114 - 143	117 - 146	110 - 139	95 - 124
band 3 (#features)	168 - 197	169 - 198	169 - 198	169 - 198

Table 3. Comparison of the quality between Algorithm 1 and Algorithm 2, using counting of miss-classified pixels.

Some of the bands found in the algorithm with the two classifiers are really different. Comparing band 1 for the Bhattacharyya distance and the Mahalanobis distance for Algorithm 2 shows that very different bands are selected, while the classification error is similar. This raises the question if there are more band combinations that give similar results. The differences in QDC classifier error are small and slightly in favour of the

Mahalanobis distance algorithms, and it is not known if these differences are really very significant. In view of these small QDC differences and the algorithm speeds described in the previous section, no positive choice for a preferable distance measure can be made.

To investigate this, the quality of all band combinations (34220 in total) has been plotted for the Bhattacharyya distance and the Mahalanobis distance. These plots offer a revealing view on the significance of 'best bands'. There are in fact a lot of different band combinations that have a quality close to the maximum value, especially in the case of the Bhattacharyya distance. The periodic nature of the figures arises from the systematic way in which the band combinations were chosen. Because of that, a certain band may occur more than once. Having in mind that there is no direct translation of the distance measure into the classification result, it makes sense to not only look at the band combination with the highest distance, but also to band combinations with bands nearby those bands. If the bands are plotted that are within 10% of the maximum value for the Bhattacharyya distance, the band around 11 μm has the highest contribution to the quality, since it is always present, see Figure 2a. When this band is chosen in combination with a band between 10 and 10.5 μm , the choice of the third band does not matter anymore. It can be anywhere between 8 and 9.7 μm . Hence the contribution of this third band is minimal to the classification result. The set of the selected bands is shown in Figure 2a.

Figure 2b shows the pixel classification results. The red line in that graph represents the classification error of the band combination with the highest quality. Its classification result is average compared to the classification when the other band combinations with quality within 10% of the maximum is being used. The blue line shows the classification errors for the band combinations of three bands selected from Figure 2a. The number of miss-classified pixels seems large but is considered over the entire image.

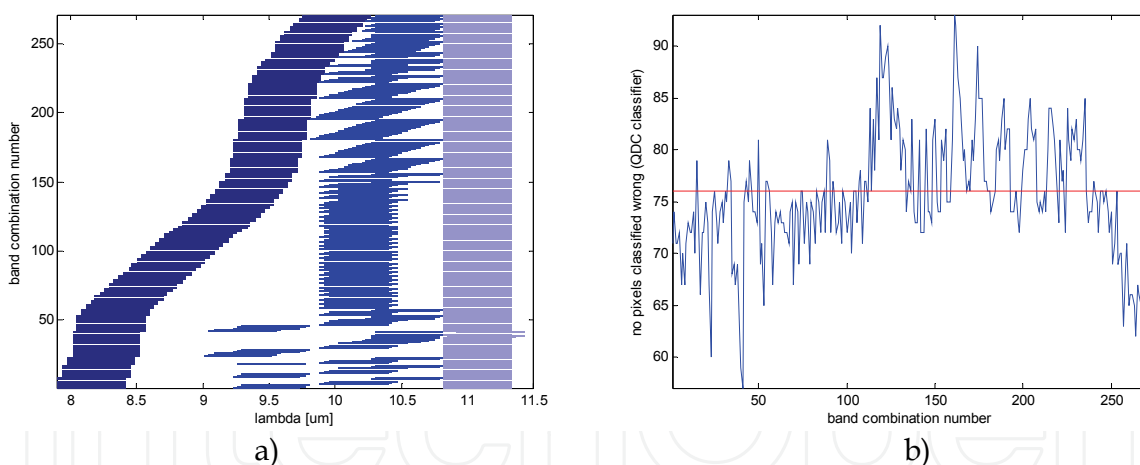


Fig. 2. Bands that have a quality (using the Bhattacharyya distance) within 10% of the maximum quality and associated miss-classifications. Figure 2a shows the combinations of three different wavelength bands of 1 μm wide, that were selected by the algorithm. Figure 2b shows the classification errors in numbers of wrongly classified pixels for these band combinations (labelled by number).

Classification results have also been compared by using the Mahalanobis distance. This time there are only a total of 26 band combinations that are within 10% of the maximum and the bands are all around the same wavelengths. Surprisingly, these bands do not show up in the set of best bands found using the Bhattacharyya criterion. Still, the bands found with the Mahalanobis criterion give a comparable classification result. Apparently, the boundary of 10% within the maximum could be set lower to include even more band combinations.

In the application of band selection a two stage process can be applied. First, based on the distance measure a first selection of best band can be made. This results for instance in the top 10 % of bands as described in Figure 2. We can then fine-tune the band selection by calculating the number of miss-classified pixels. This process requires the use of the ground truth information or user supplied inputs. In the case of Figure 2 this would result in selecting the minimum number of miss-classified object pixels, hence the band combination 40. In this way we optimize the miss-classifications for the requested limited set of three bands.

2.4 Applications of band selection

Reasons for band selection can be processing speed, or as in our case display capability. The selection of three bands allows for easy display on the RGB channels of standard displays. In the learning phase of the band selection process of band selection, an effective visualization tool is essential to understand the steps taken by the tool. In this way the operator has a better understanding of the information content in the bands that the algorithm selects.

The number of required spectral bands is assessed with the approach described in the previous section in a number of steps in a Matlab® environment. The first requirement is that the user has to input a hyperspectral image cube in which target and background are present. Subsequently regions in the image are selected and attributed to either background or target. Target boxes are coloured in red, background boxes in white. When all relevant target and background areas are selected the spectra of all pixels inside either the target or the background boxes are plotted at the bottom panel of the graphical user interface (for this GUI see Figure 3).

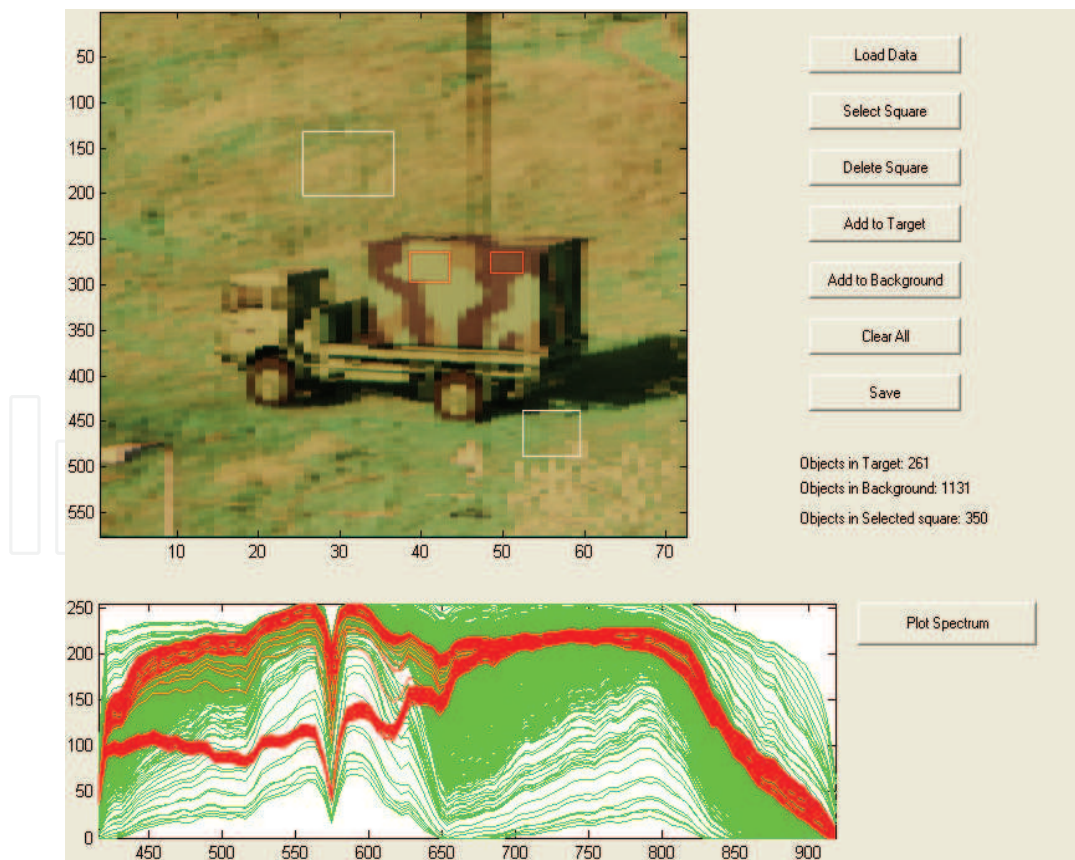


Fig. 3. Spectra from target (red lines) and background (green lines) locations in the image, and spectra of target areas and background areas are selected via this Matlab® GUI.

Within the feature (here specified as a spectral band) selection tool the feature width and the maximum allowed overlap are input. Now the optimum position of these features is calculated. The result of the optimum band positions is plotted in the top panel of the GUI (see Figure 4), by vertical lines that are drawn over the spectra. Each band starts with a blue vertical line and ends with a black vertical line. The optimum spectral band positions are also outputted to the Matlab® command line.

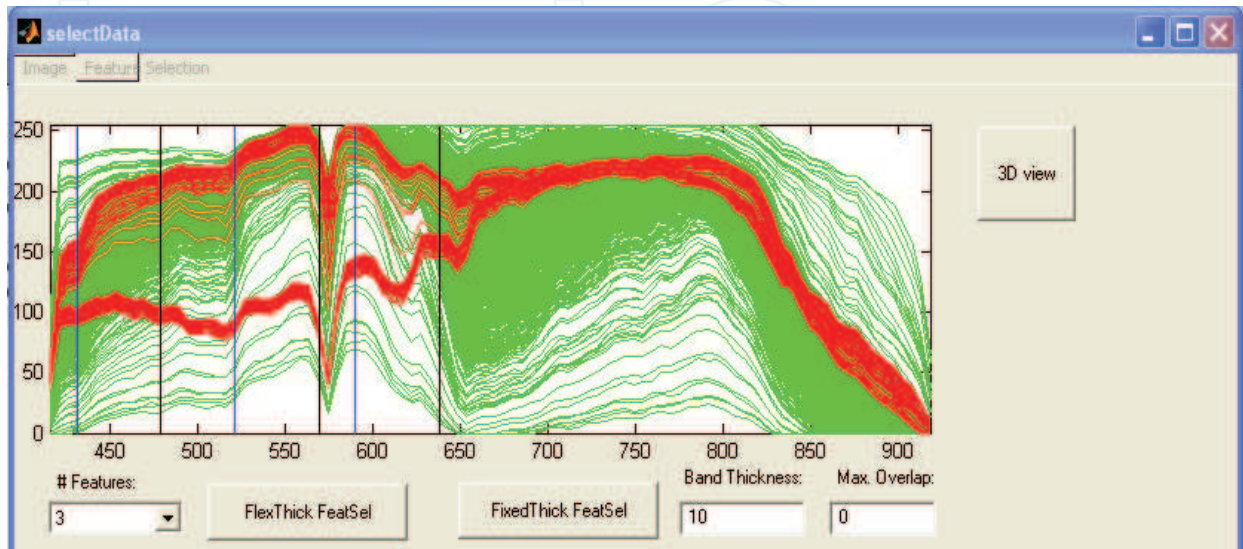


Fig. 4. Optimum position of spectral bands are indicated by vertical lines. Blue lines mark the start of the new band, black lines mark the end of the band.

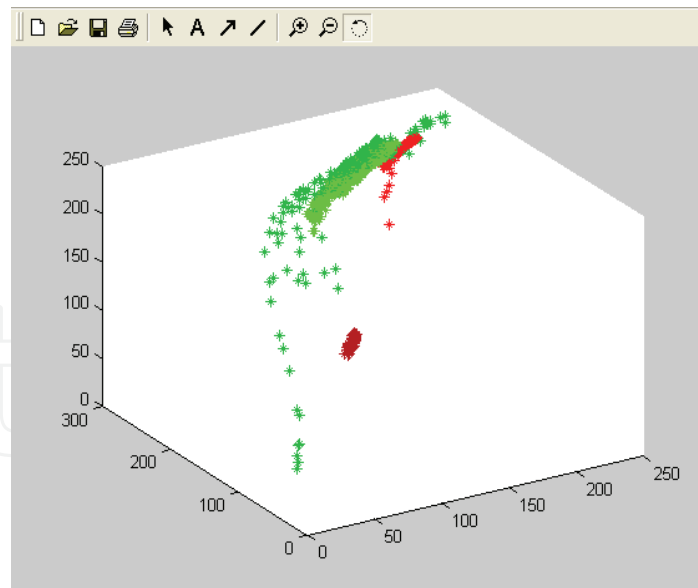


Fig. 5. Projection of pixels in 3-dimensional space spanned by three selected features (spectral bands).

If exactly three features (hence three bands) are selected the position of the pixels in 3-dimensional feature space are plotted (see Figure 5). The user can rotate the cube to inspect the separation that has been achieved between target and background pixels using the selected number of features.

2.5 Conclusions and discussion on band selection

We have presented an effective approach for optimal band selection of hyperspectral data. Our approach, named HYBASE, is typically used in a system design study and these outputs can feed operational studies. Figure 6 shows the location of the HYBASE tool in this design chain. Based on a hyperspectral data set in a relevant scenario one can make an analysis with this tool of the minimum number of required spectral bands, their widths and positions for the targets/backgrounds.

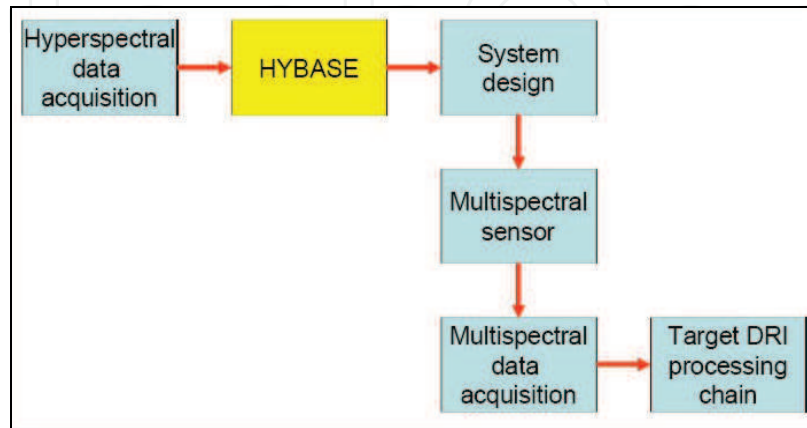


Fig. 6. Typical usage of the HYBASE base spectral band selection tool in system design.

First, the acquired hypercubes are being pre-processed using geo referencing, noise reduction, data normalization, temperature emissivity separation etc. Then, targets are being detected using anomaly and signature based detection method in combination with change detection. Spatial information is used to reduce false alarm rates. Additional sensor data from e.g. high resolution imagers, radar and/or 3D laser radar is used to classify and identify targets in a decision fusion process. Many of these algorithms run near real-time. Potential applications of sensor combinations are described in Schwering et al. (2007).

Below we will describe the main conclusions of our analysis. One has to keep in mind that these conclusions are based on an analysis using only one dataset with a frequency range from 7.7 μm to 12.1 μm (i.e. mainly emissivity is measured):

- Algorithm 1 (the fast band selection algorithm) performs good compared to Algorithm 2 (the optimal algorithm). The band combinations found by Algorithm 1 have a quality value within 15% of the quality found by Algorithm 2, while the calculation time is a lot smaller.
- Using the Bhattacharyya distance as a measure for the separation of the different classes gives comparable results as the Mahalanobis distance.
- Although no thorough study has been done between the relation of the quality and the classification error, in some cases the difference in classification error can be very large for similar qualities (up to 100% difference).
- Often, there is a whole set of different band combinations that have a comparable quality and classification result. This set is revealed by plotting the band combinations having a quality within a certain percentage of the maximum quality.
- As a consequence of the above two points, the band combination with the highest quality does not necessarily have the lowest classification error.
- The location of the best bands depends strongly on the choice of target and backgrounds.

- For a good classification result clean spectra of the targets are required. Target masks for semi-hidden targets are useless, since they contain target as well as background pixels.
- If the number of bands increases the quality increases and the classification error decreases. Although other research shows that there is an optimal number of bands for the classification error, this did not show up in our results. This optimum is due to the fact, that when the number of bands increases, statistical values used to describe the feature-space like the covariance matrix can be predicted less accurate. That this optimum did not turn up in our results is probably due to the fact that we classified areas that were also used to train the classifier.

We found no clear relationship between the bandwidth and the quality. The influence of the bandwidth on the quality is substantially less than the influence of the number of bands. This is probably because the spectra in the thermal infrared region ($7.7 \mu\text{m}$ to $12.1 \mu\text{m}$) involved did not have any sharp features.

If the complete hyperspectral image cube has to be processed the huge amount of data of a hyperspectral image cube is troublesome. This complicates a near real-time image processing solution. Band selection is an important step in realizing operational hyper/multi spectral imaging solutions. In Figure 7 we present a potential processing chain for automatic target data processing of hyperspectral image information. This describes the complete system, consisting of various real-time on-line steps, combined with supporting off-line data mining activities (represented by the history block).

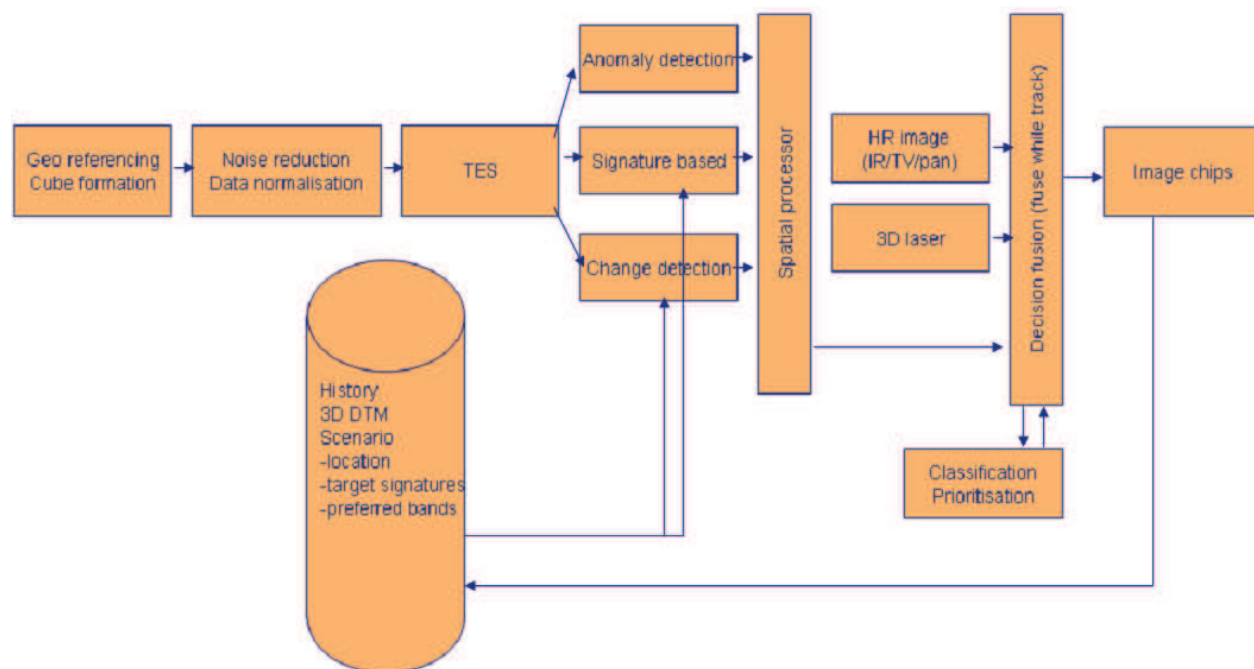


Fig. 7. A potential approach to a multi spectral image processing chain. Recorded data is put in the chain from the left, and follows each process represented in the blocks, finally resulting in image chips.

Most research involving band selection has focussed only on the location of the bands. However, for a multispectral configuration very narrow bands are not practical, because this would require large integration times to get a good signal-to-noise ratio. Our research therefore not only looked at the location of the bands but also at the width of the bands.

3. Visualisation

In automatic target detection a distinction can be made between anomaly detectors and spectral signature-based detectors. The former assume no a-priori information about the target spectral signature and simply detect those pixels that have a spectral behaviour anomalous with respect to the surrounding, global or local, background. The latter rely on the fact that the spectral reflectance of the target is known (e.g. by ground or laboratory measurements) and assume that the atmosphere can be accurately modelled in order to predict the spectral radiance expected at the sensor level. Of course, atmospheric modelling is critical and poses serious limitations to the application of this kind of algorithms in operating conditions. Nonetheless, spectral signature based detectors allow target recognition while anomaly detectors simply detect the positions of candidate targets (target cueing). In this latter case a further step is needed to mark those regions that possibly contain a true target. Furthermore, when a human observer (instead of an automatic system) interprets the data, the presentation type that suits the application best depends on prior knowledge. Our main focus is on (potential) target detection without prior knowledge. We present four new visualisation methods. These methods are evaluated in an experiment in which human observers were required to detect a number of targets.

For evaluation purposes two hyper spectral images (hyper cubes) are used obtained by an airborne hyper spectral sensor operating in the visible and NIR (near infrared) domain. It has a high spatial resolution resulting in a pixel size of approximately 0.3 meters and 160 spectral bands in the range from 0.4 μm to 1.0 μm . The targets consist of commercially available camouflage nets. The data sets were recorded in a rural environment containing mainly forest, grass and bare soil. The two hyper cubes used in this study are referred to as set A and set B. The two data sets were acquired from the same altitude (1000 m) and along the same (nominal) route. Set A was recorded in clear weather conditions around noon and set B was recorded in overcast conditions at about 6:00 pm. The datasets are 414x317 (A) and 500x307 pixels (B).

3.1 Presentation methods

We will discuss various presentation methods some of which rely on more prior information than others. The focus is on unsupervised target detection. The hyper spectral image is a 3-D data set M_{ijk} , in which i represents the (spatial) y-dimension, j the spatial x-dimension and k the index of the band (representing the wavelength dimension).

3.1.1 Broadband signal

The average over all bands can be regarded as the baseline signal. In formula (with N_k the number of bands)

$$A_{ij} = \sum_k M_{ijk} / N_k \quad (4)$$

An advantage of viewing the average signal is that the noise is low relative to the noise in the separate bands. It is therefore advisable to inspect the average signal, especially when the amount of noise in the image is relatively large. The resulting image is similar to that of a broad band sensor.

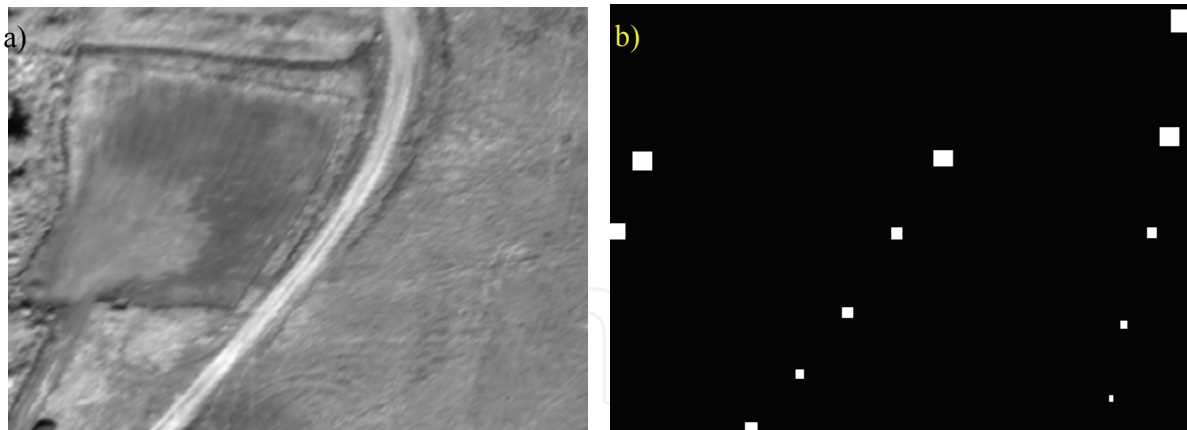


Fig. 8. Average signal of sample set A (a) and designated target locations (b).

Figure 8a shows an example of a broadband signal (set A). The designated targets are depicted in Figure 8b. In the broadband signal some targets may be visible while others may remain invisible because much of the potential target information in the data set is unavailable.

3.1.2 Movie presentations

When the hyper spectral data cube is displayed as a movie sequence all bands can be displayed. In principle there is no loss of information. In practice there are limitations to the temporal and spatial processing capabilities of the visual system which have to be taken into account when designing a good presentation form. A useful property of the data is that the (meaningful) signal varies slowly from band to band (in most cases). This means that rapid variations can be regarded as noise. When the raw data is displayed as a movie sequence the movie is almost indistinguishable from the static image of the average output. This is due to the fact that (in our case) the spatial variation between pixels is much larger than the band-to-band (wavelength dependent) variations in the output. We expect that this is a common property of hyper spectral data sets.

A solution to this problem is to subtract the average output value (of each pixel; Av_{ij}) from the output of each band and display this difference ($D_{ijk} = M_{ijk} - Av_{ij}$) as a movie sequence. In a previous study (Hogervorst & Bijl, 2006) using different hyper spectral data this method was successful in revealing many of the designated targets visible. However, with the current data this method did not work, due to the fact that pixel to pixel variations overruled the (much smaller) band-to-band variations. To make these spectral differences between pixels more visible we developed another method. We found that the difference-from-average signal D_{ijk} of each pixel is well modelled by a factor (f_{ij}) times the average profile (F_k):

$$D_{ijk} = f_{ij} \cdot F_k + \varepsilon_{ijk} \quad (5)$$

Figure 9a shows the difference-from-average (D_{ijk} , $i = 1$, $j = 1$) of the top-left pixel as a function of band index along with a scaled version of the average profile ($f_{ij} F_k$). The signal of the individual pixel (solid line) closely follows the scaled average profile (dashed line). Figure 9b shows the deviation (ε_{ijk}) from this model (solid line). Also shown is a version in which the band-to-band noise is reduced (dashed line). Although reduction of band-to-band noise is not strictly necessary, since the human visual system is highly robust to noise, it is more comfortable for the user. Standard noise reduction techniques can be applied to reduce the noise. We filtered the spectral signal with a Difference-of-Gaussians kernel (DOG) given by $2 \cdot \text{Gauss}(\sigma) - \text{Gauss}(\sigma\sqrt{2})$ (see inset Figure 9b), with $\sigma = 2$, to get rid of the high frequency

modulations ($Gauss(x, \sigma) = 1 / \sqrt{2\pi\sigma^2} \exp[-(x^2 / 2 / \sigma^2)]$). We used no spatial filtering to reduce the noise, since this would obscure small targets. The underlying assumption is that the fast fluctuations in the signal are due to noise. In cases in which this assumption is not appropriate information is lost by using noise reduction methods. This is the case when peaks in the signal are meaningful. In practice the width of the filter should be based on a prior analysis of the noise (preferably by inspection of a constant reference sample).

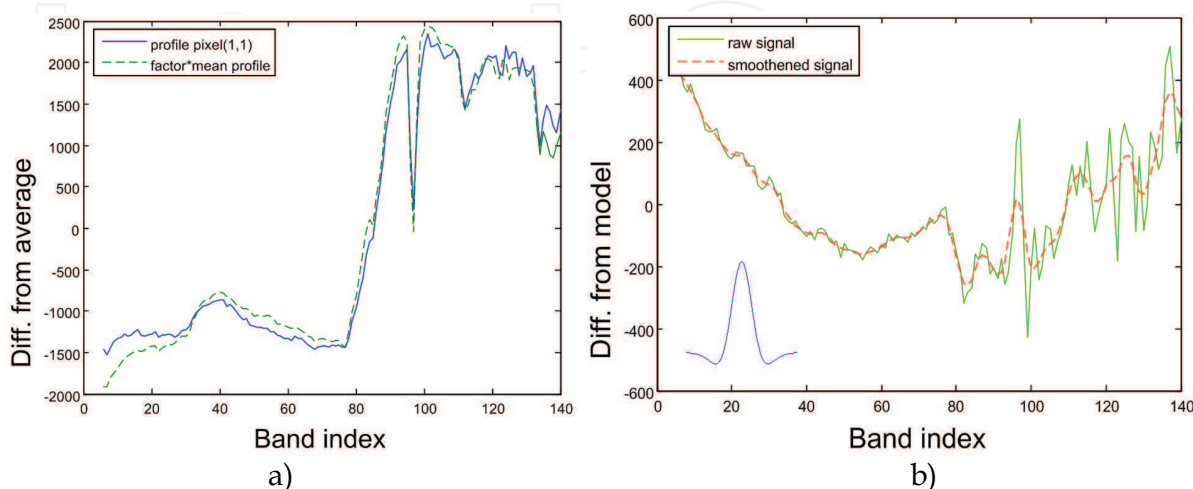


Fig. 9. a) difference-from-average output for pixel (1, 1) (top-left pixel; solid line) along with a scaled version of the mean profile (factor * mean profile; dashed line) of the difference-from-average signal. b) the deviation from the scaled average profile (solid line). This is the difference between the signals shown in Figure 9a. Also shown is a version in which the band-to-band noise is reduced (dashed line). This signal is obtained by filtering the raw signal with a Differences-of-Gaussians-kernel (see text); the filter shape is shown as an inset in Figure 9b.

Figure 10 shows three frames of a movie sequence containing the deviations from the scaled profile (see Figure 9b). In the first and last of the three example frames no targets are visible. In the middle frame most of the targets are visible. This shows the advantage of using a movie sequence as a presentation technique. Ideally, when the differences are apparent in (at least) some of the frames, this information will be picked up by the observer. Differences in spectrum between the targets and the background become apparent as a difference in the temporal profile. Furthermore, human observers take into account the fact that targets differ from elements in the background in shape and size.



Fig. 10. Three frames of a movie sequence showing the differences from average for band indices 6, 34 and 52. The targets are invisible in bands 6 and 52 but visible in band 34. In this case we also applied dynamic noise reduction in which the temporal noise is reduced (see text). This latter transformation is not strictly necessary since the human visual system is highly robust to noise.

3.1.3 Colour schemes

The colour presentation technique produces a single image. In this case all bands of the hyper spectral signal are mapped to three independent channels. We tested several different colour schemes. In the first scheme the hyper spectral data set is divided into three broadband signals. First, the three broadband images are deduced and mapped onto the range (0, 1). Then, the average over the three images is calculated and subtracted from the broadband images. The reason for this is that (in our case) the average signal does not contain much information about the targets (see e.g. Figure 8). The difference images are then mapped onto the range (0, 1). Finally, the three (difference) images are fed into the Red, Green and Blue channels of a colour image. In a previous study (Hogervorst & Bijl, 2006) using other hyper spectral data sets this method worked quite well. However, in the current study this method did not reveal the targets. This is not surprising since a movie sequence showing the differences from the average output described in the previous section did not show the targets either. Therefore, a second data transformation was developed in which differences from the scaled average profile (see section 3.1.2 and Figure 9) are used. First we tried to apply the method described above for transforming the data into a colour image. This also did not result in an image revealing the targets. The reason for this is that this signal fluctuates rapidly from band to band from positive to negative values. So, the signal averages out in the broadband channels.

To map the signals onto a colour image we therefore resorted to a different method. We apply a principle component analysis to the (differences-from-scaled average profile) data set. The main three components are mapped into HSV-space (hue, saturation, and value components). Finally, the HSV data is transformed into an RGB-image and displayed. Figure 11a shows the result of this transformation.

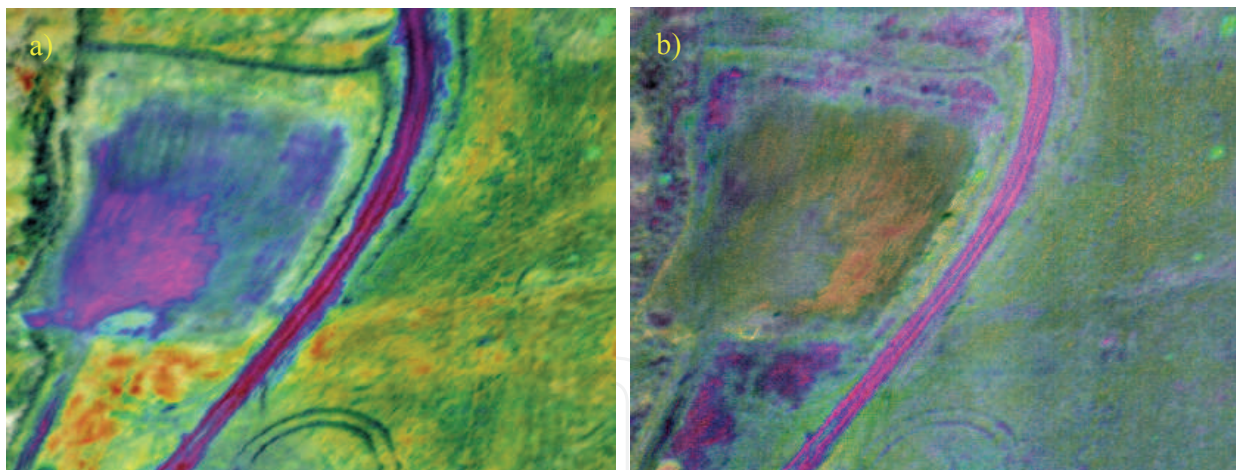


Fig. 11. a) a colour representation using the first three principal components of the differences-from-scaled average profile. The components are used as HSV-signals and converted into RGB. b) similar presentation using principal components 4, 7 and 8 (see Figure 12).

The result of the principle component analysis is interesting in its own right. Figure 12 shows the first 16 principle components. Figure 12 shows that the useful information in the hyper spectral data set (containing 160 bands) is limited to a small number of independent components (smaller than 16 in our case). With increasing component index the amount of noise increases. The targets appear in some of the components. Also visible in some of the components is fixed pattern noise with the shape of a sinusoidal corrugation (e.g. in components 5 and 6).

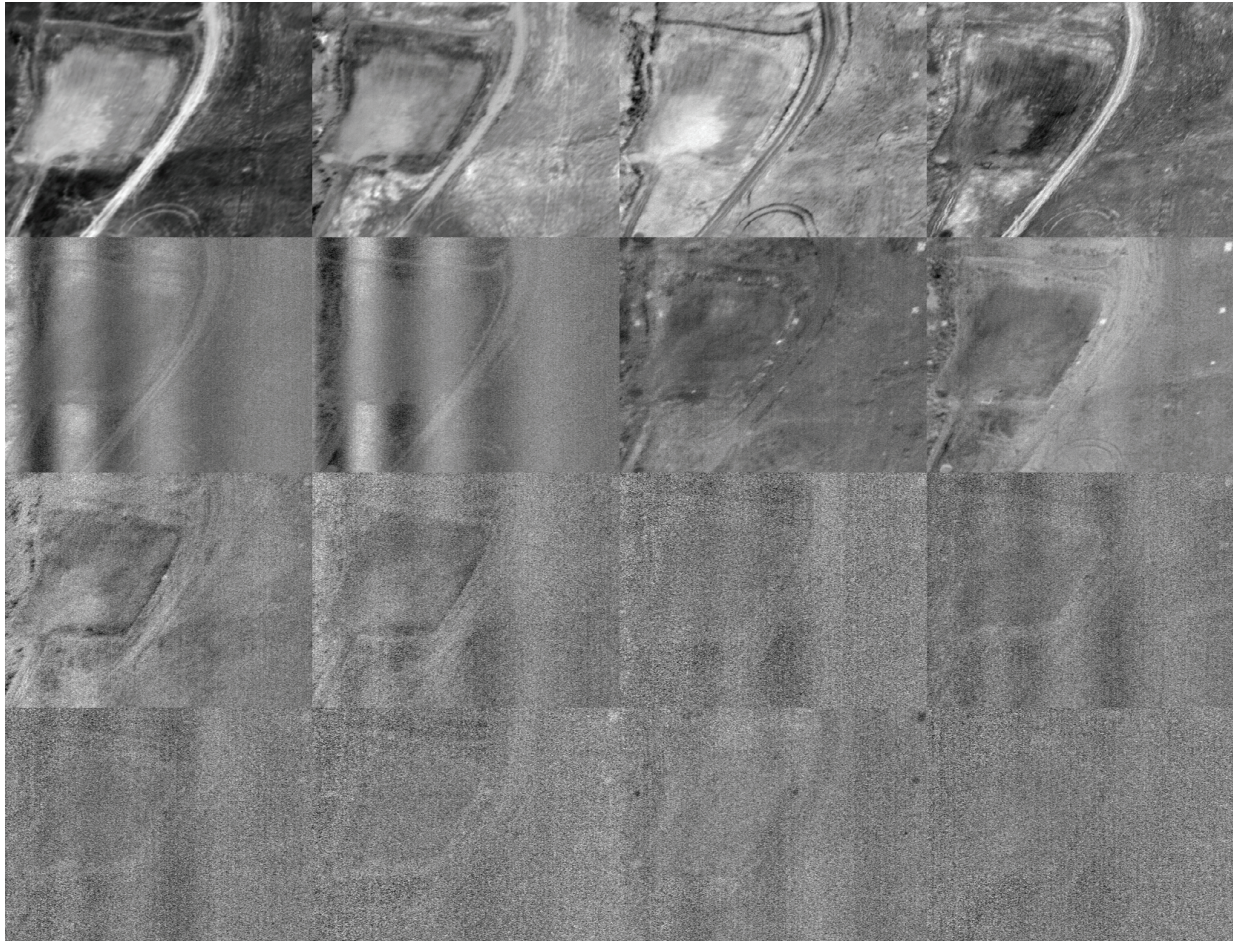


Fig. 12. First 16 principle components of difference from model (scaled average profile) data. The information content is limited to several bands: the amount of noise increases with the component index.

Which three components to combine into a colour image is difficult to decide beforehand. By default we use the first three components (Figure 11a). A more optimal combination may be found for these targets (Figure 11b). Since it is not clear from the start what the targets look like it seems reasonable to inspect all useful principle components for (potential) targets. In the evaluation experiment the default colour scheme (using the three main components) was used (assuming no prior knowledge about the targets). An alternative would be to present all informative principle components as a movie sequence, such that the loss of information is reduced.

The disadvantage of the colour scheme is that some information is lost. The advantage of this presentation type is that it can be displayed as a single image and is therefore suitable for real time presentation.

3.1.4 Signature match

When the spectral signature of the target is (reasonably) well known it can be used to highlight the target in the image. A wide range of spectral signature matching techniques exist (e.g. Green and Craig, 1985; Kruse et al., 1985; Yamaguchi and Lyon, 1986; Clark et al., 1987), which try to capture the characteristic properties of the spectral signature (e.g.

locations of steep slopes). Image spectra can be compared with individual spectra or to a spectral library (Kruse et al., 1993). This often requires calibrated hyperspectral image data in which the data is reduced to the apparent reflectance (true reflectance multiplied by some unknown gain factor).

Here, we calculate the resemblance between the signature of each pixel and that of a target. As in previous sections we use the difference-from-scaled average profile as the basic data set. We calculate the correlation between the signal of each pixel and that of the target signal. We take the average signal of the top-right target (see Figure 8b) as the target signal. The result is displayed in Figure 13a. Since (in this case) all (designated) targets have similar profiles many of the targets show up in the image. This method is well suited for finding targets with profiles similar to the one that has been identified (by inspection or prior knowledge, i.e. supervised classification). Of course, one can also look for multiple targets with different profiles simultaneously.

3.1.5 Anomaly detection

The task of the observer is to indicate (potential) targets without prior knowledge of the target or background signatures. This is similar to the task faced by an anomaly detector. We used a standard RX-detector as developed by Reed and Yu (1990) to calculate the degree of anomaly. This detector is commonly used to detect targets whose signatures are distinct from their surroundings. Instead of resorting to automatic detection, the interpretation of the data is left to a human observer.

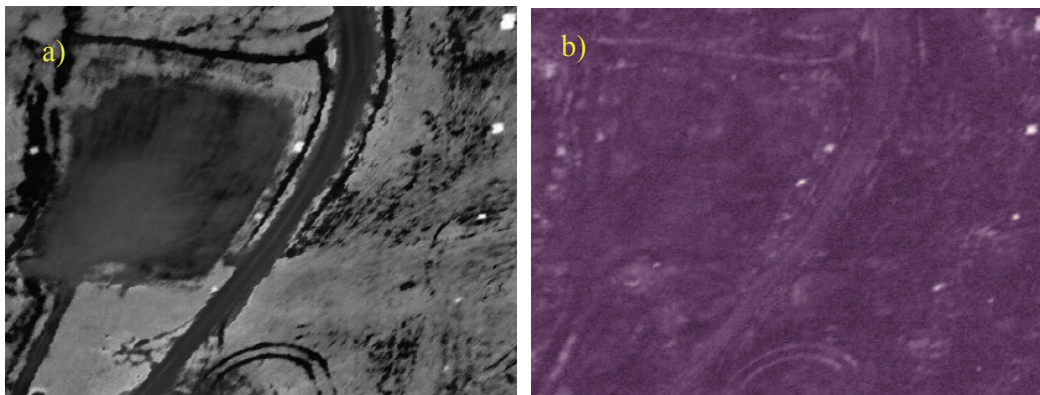


Fig. 13. a) Correlation between pixel signature and target signature (using the difference-from-scaled average profile data). b) Output of the RX-detector.

In our implementation of the RX detector a dual window was used to estimate the background mean vector and covariance matrix. It consists of a guard window that should match the size of the maximum expected target and an outer window where the training samples are collected. The following parameters were used. For data set A we used an inner window size of 71 pixels and an outer window size of 75 pixels. For data set B we used an inner window size of 80 pixels and the outer window size of 84 pixels. Figure 13b shows the output of the RX-detector for data set A.

3.2 Evaluation experiment

3.2.1 Method

Two data sets were used, referred to as set A and set B which were registered by the hyperspectral sensor described in section 3.1. We compared performance for detecting targets for 4 different presentation techniques:

- Movie
- Anomaly
- Match
- Colour

The experiments were carried out in a dimmed room. Subjects were seated in front of a 22 inch CRT-monitor (40x30 cm, 1280x1024 pixels) with a refresh rate of 75 Hz and a monitor-gamma of 2.2. Twenty four subjects participated in the experiment. Each subject was shown data sets A and B using two distinct presentation types. All combinations of presentation types and presentation order were used. The data was balanced with respect to presentation order and combination of presentation types. Each session started with an instruction showing all presentation types. In this instruction a data set was used that differed from the ones used in the experiment. The subject was told that the images represented airborne images of a natural environment containing targets. We also told the subjects that potential targets were characterized by the fact that their spectrum differs from that of the background, and that the targets differ in shape (are restricted in size) and form from background elements. They were also told that the number of targets could be anywhere between 1 and 20. The task of the subjects was to indicate potential targets by clicking the mouse in the chosen locations.

In some cases the subjects picked the same location more than once. In our analysis we treated locations less than 8 pixels apart as the same target, and the average location was used as the perceived target location.

3.2.2 Results

Figure 14 gives an overview of the performance for the different presentation types. Shown are the hit-rate and one minus the false alarm (FA) rate, in which the hit rate corresponds to the number of indicated targets divided by the total number of targets, and the false alarm rate corresponds to the number of false alarms divided by the total number of indications. Two-sided student-t tests on each of the separate data sets (A and B) were carried out (using the individual hit- and FA-rates) to determine which pairs of conditions differed significantly from each other (at a significance level of $p = 0.05$).

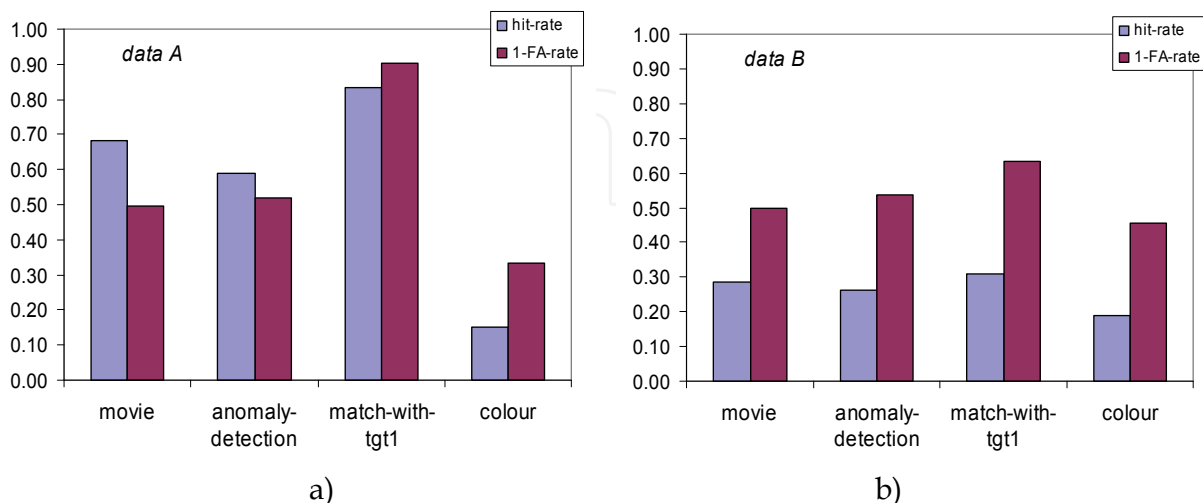


Fig. 14. Overall performance measures HIT-rate and 1 - FA-rate (one minus false alarm rate) for the different presentation types for data sets A and B.

The best performance was found in the condition showing the match between pixel and target signature (of the top-left target), with the highest hit-rates and lowest FA-rates. Pair wise comparisons show that the hit-rate in this condition is significantly higher than the hit-rate in the “anomaly detection” and “colour” conditions in set A, while in set B the hit-rate significantly deviates from the “colour” condition. The FA-rate in this condition is significantly lower than the FA-rates of all other conditions in set A. In set B we did not find any significant differences in the FA-rates of the conditions. The “match” condition relies on prior knowledge of the target signature. This may be obtained through analysis of the data using a different presentation type. Alternatively, the target spectrum may be known from other sources of information. The results show that this information (whenever available) can be used to increase performance.

Performance in the “colour” conditions was the poorest. Pair wise comparisons reveal that the hit-rate in this condition is significantly lower than the hit-rate in all other conditions in set A, and significantly lower than the hit-rates in the “movie” and “match” conditions in set B. Also, the FA-rate is significantly higher than the FA-rate in the “match” condition in set A.

Intermediate performance was found in the “movie” and “anomaly” conditions. The hit-rate for the “movie” type is somewhat higher than that for “anomaly”, but the FA-rate is also somewhat higher, although these differences are not significant. The combination of a higher hit-rate and higher FA-rate is consistent with the fact that in the “movie” condition the number of indications is higher (on average about 19%) than in the “anomaly” condition. The number of indications was found to be the largest in the “movie” condition, followed by “anomaly”, “match” and “colour” conditions.

Figure 15 shows the hit-rate per target. The targets are ordered such that the average hit-rate decreases with increasing target number (set A contains 14 targets and set B contains 11 targets). Some targets are detected with (almost) all presentation types, other targets are never detected, while some targets are only detected with certain presentation types. As noticed before, hit-rate increases from “colour” to “anomaly” to “movie” to “match”.

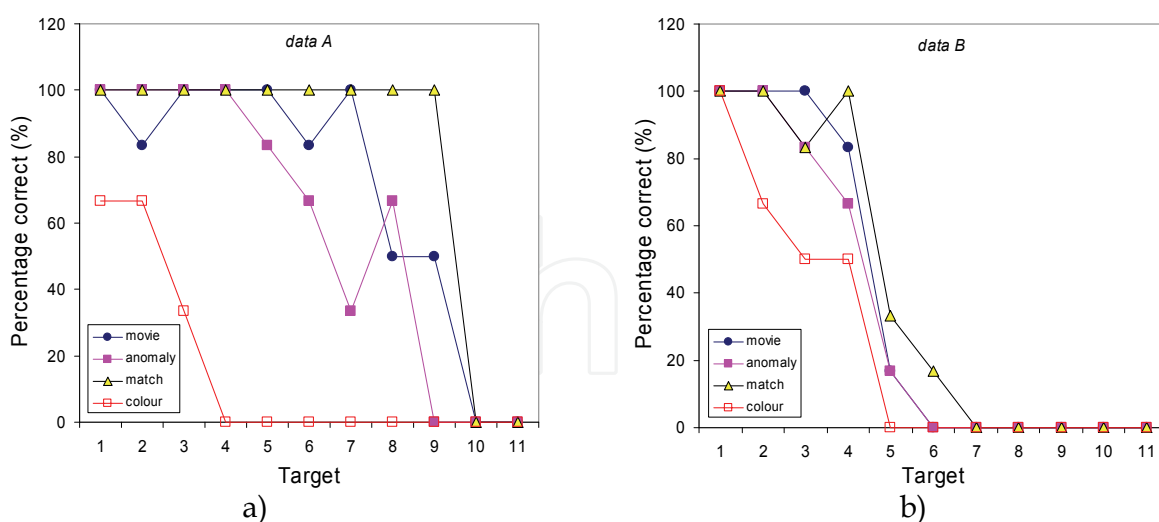


Fig. 15. Hit-rate per target for the different presentation types for data sets A and B. The targets are ordered according to difficulty of detection.

Figure 16 shows the densities of target indications for the various presentation types, along with the designated target positions for data set A. This figure shows that some areas consistently act as false targets. Also, some of the targets are missed by all of the subjects (see also Figure 15).

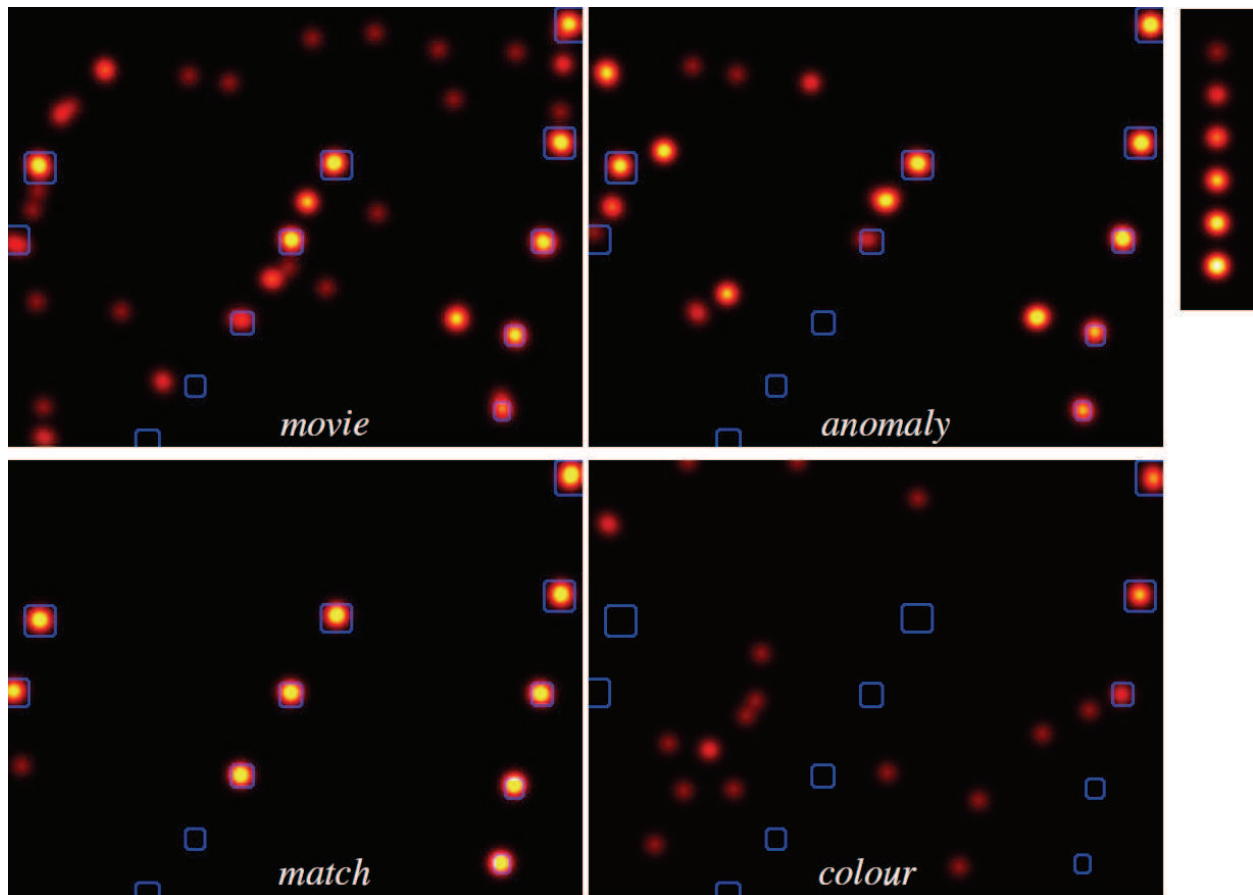


Fig. 16. Density graphs showing the density of target indications for the 4 different presentation types for data set A (for set B: see Appendix). The (blue) borders indicate the designated target positions.

3.3 Conclusion and discussion visualisation

We have presented four new methods to visualize hyper spectral data for human target detection. The human visual pattern recognition system is exploited to find potential targets and to decide whether a certain image detail is a potential target. The advantage of relying on human interpretation is that the human visual system is highly robust to noise and image transformations such as drift, translation and distortion. For instance, when the sensor (or parts of the environment) moves while the hyper spectral data is recorded, the pixels in the various bands will not be in correspondence. Automatic target recognition algorithms will have a difficult job in finding the targets in this case, while this does not represent much of a problem to the human visual system.

The first presentation type we developed is referred to as the “movie” type. In this presentation (transformed versions of) the different bands are shown in sequence. In principle no information is lost in the transformation process. The method does not rely on specific assumptions about the target signature. Its effectiveness however relies on the way the data is transformed before display. This determines whether the information in the data can be picked up by the human observer. For instance, a movie displaying the raw data looks very similar to the average broadband signal. This is due to the fact that the spatial variations are often much larger than the differences in the band-to-band variations between pixels, effectively overriding the spectral information. To overcome this problem the data

was transformed (using the deviations from the scaled profile) to make the differences more visible. By applying noise reduction a clearer movie sequence can be created. This may not be strictly necessary since the visual system is well capable of discarding the noise. Even so, noise reduction can make it easier to interpret the data and may lead to faster responses, better visual comfort and less fatigue. The downside is that noise reduction removes small details from the image. In cases in which these small details contain meaningful information (this type of) noise reduction is not appropriate. For the same reason we did not use spatial averaging, since this makes it more difficult to detect small targets.

The second presentation type we investigated was the “colour” type. The advantage of such a presentation is that it results in a single image, and can therefore be used to present the data in real-time (on-the-fly). However, because a colour image contains only three independent channels, some information is lost and a suitable choice of channels has to be made. Again, the pre-processing steps in creating the colour image crucially determine whether the targets will be visible. One option is to use three broadband channels which are used as input to the RGB-channels of an image (e.g. using the result of the band selection algorithm described in section 2). As in the movie type presentation, we used the difference-from-scaled average profile as the basic data set. We applied principle component analysis to this data and used the three main components to create a colour image. This results in an image that shows only some of the targets. In general, the three (broadband) channels used for creating the colour image should be tailored to the signature of the targets and the background. The images resulting from the principle component analysis are useful for target acquisition in their own right and can be used to tailor the colour scheme to a particular set of targets. What presents the optimal colour scheme also depends on the application. Detection and identification performance depends on the distribution of noise among the different colour channels (Bijl et al., 2005). Situational Awareness benefits from naturally looking colour schemes (Toet, 2005).

The third presentation type we investigated was “anomaly detection”. This method relies only on a few assumptions. The size of the targets has to be known reasonably well, although the output is not too critically dependent on this. We used the standard RX-detector (Reed & Yu, 1990). A difference with the way it is commonly used is that here the interpretation is left to a human observer (aided target detection), who can take into account the shape and size of the (potential) target. In contrast to most automatic detection algorithms the human observer does not merely analyze the output of individual pixels, but takes the context into account.

The fourth presentation type we analysed was a presentation showing the “match” between the signature of each pixel and the target signature (using the difference-from-scaled average profile data). The method relies on the fact that the target signature is known a priori. It can also be used to find targets with similar signature once one target has been identified (e.g. from using a different presentation technique). Targets with similar signature become clearly visible. The disadvantage of this method is that targets with a different signature are not revealed by this method. Of course, a match presentation can be derived for various different target signatures. These representations may be combined in a movie type presentation or by the use of colour (e.g. displaying the result for 3 target signatures).

The four presentation types were evaluated in a human observer experiment. This showed that the “match” presentation led to the best performance, with the highest hit-rate and lowest false-alarm-rate. This result was expected since all targets had similar signatures (this

does not hold in general). Performance with the “colour” presentation was found to be quite poor (poorer than in a previous study: Hogervorst & Bijl, 2006). One reason for this is that the default colour scheme was used (with the three main principle components) to prevent the use of prior knowledge. A more optimal colour scheme may be determined that is geared at these targets, e.g. by using PCA (see e.g. Figure 11b). With the “movie” presentation the hit-rate was higher than in the “anomaly” presentation, but the false-alarm-rate was also somewhat higher. Which presentation type is better to use in general is difficult to decide. This will also depend on the cost associated with a hit and a false alarm. In principle, the movie sequence contains more information. However, it seems to be harder to interpret (and may be improved by training). On the other hand, the result of the anomaly detection can be displayed in a single image and is therefore more suited for real-time display.

Noise can sometimes override the signal in the separate bands of a hyper spectral sensor. In hyper spectral systems there is a trade-off between the number of bands and the noise in each band. The noise in a hyper spectral system effectively limits the useful number of bands. We have found that an indication for the number of useful independent bands can be obtained from PCA (in our case only about 10 useful independent components remain). An advantage of a hyper spectral system over a fixed broadband system is that the user can decide how to combine the information across bands (see section 2).

In order to improve search performance by prior knowledge, one may start a search by recording the signature of targets similar to the ones that one tries to find (although this may lead to a loss of targets with signatures that differ from the recorded ones). In this way, one can tune the system to the targets of interest without the need for calibrated data (which required compensation for atmosphere, etc). Similarly, it is advantageous to record the signatures of various types of background. Such information can help in tailoring the system to the interesting targets.

Some presentation types are more suitable for real-time processing (e.g. the colour scheme) and some schemes are more suitable for post-hoc analysis (e.g. the movie type). Still, schemes of the second type can be applied immediately after recording. Some of the presentation types rely more heavily on knowledge about the target than others. It is advisable to use more than one presentation type to be sure that certain information is not overlooked (e.g. in the average image) and all available information is used (and unexpected targets are not missed).

4. Overall summary

Hyperspectral sensors are used in an increasingly wide range of applications. The data contains a wealth of information. The challenge is to extract this information. Also, the question is to what extent hyperspectral data improves task performance and whether it can be approximated by a more simple multi-band sensor system. We have presented a method for choosing the bands (width and position) that result in as limited information loss as possible. Such a band selection tool is essential in the design of multispectral sensor systems, and may be used as an initial stage in data processing to reduce the amount of data. In our case, band selection optimizes the target-to-background contrast (relevant for target acquisition performance). We have described our algorithm and presented an evaluation by

applying it to a representative dataset. We have also presented and evaluated different ways to visualise hyperspectral data. The various presentation types differ in the way the information is displayed and in the way information will be picked up by the observer. In a target detection experiment with human observers performance was measured and the various presentation techniques were compared. The various presentation methods vary in their optimum application, depending on the (prior) knowledge available, and whether the data is presented in real-time or used for post-hoc analysis.

We argue that often the final interpretation is best left to a (trained) human observer. Thus, the number of assumptions (signature of target and background, target shape etc.) can be restricted. Human interpretation is robust to noise and many image transformations, and can take the target background into account. Whenever knowledge about target and background (signature, shape etc.) is available this can be used to help improve the interpretation of the data by the observer (aided target detection).

5. References

- Bijl, P., Lucassen, M.P. & Roelofsen, J. (2005) Identification in static luminance and color noise. *Proceedings of SPIE 5784*, 35-41.
- Briottet X, Boucher, Y., Dimmeler, A., Malaplate, A., Cini, A., Diani, M., Bekman, H., Schwering, P., Skauli, T., Kasen, I., Renhorn, I., Klasen, L., Gilmore, M., Oxford, D. (2006), in *Targets and Backgrounds: XII, Characterization and Representation*, ed. W.R. Watkins, D. Clement, SPIE Vol. 6239-paper163, Orlando Florida (USA)
- Clark, R. N., T. V. V. King, and N. S. Gorelick, (1987), Automatic continuum analysis of reflectance spectra: in *Proceedings, Third AIS workshop, 2-4 June, 1987*, JPL Publication 8730, Jet Propulsion Laboratory, Pasadena, California, p. 138-142.
- Green, A. A., and M. D. Craig, (1985), Analysis of aircraft spectrometer data with logarithmic residuals: in *Proceedings, AIS workshop, 8-10 April, 1985*, JPL Publication 85-41, Jet Propulsion Laboratory, Pasadena, California, p. 111-119.
- Hogervorst, M.A. & Bijl, P. (2006) *Visual analysis of hyperspectral images*. Report TNO-DV 2006 A338 (STG. Confidential). Soesterberg, The Netherlands, TNO Defence, Security and Safety.
- Kruse, F. A., G. L. Raines, and K. Watson, (1985), Analytical techniques for extracting geologic information from multichannel airborne spectroradiometer and airborne imaging spectrometer data: in *Proceedings, International Symposium on Remote Sensing of Environment, Thematic Conference on Remote Sensing for Exploration Geology, 4th Thematic Conference, Environmental Research Institute of Michigan, Ann Arbor*, p. 309-324.
- Kruse, F. A., A. B. Lefkoff, J. W. Boardman, K. B. Heidebrecht, A. T. Shapiro, J. P. Barloon, and A. F. H. Goetz, (1993), The spectral image processing system (SIPS) - Interactive visualization and analysis of imaging spectrometer data: *Remote Sensing of Environment*, v. 44, p. 145-163.
- Landgrebe, D.A., (2003), *Signal Theory Methods In Multispectral Remote Sensing*, Hoboken, NJ: Wiley

- Reed, I.S. & Yu, X. (1990) Adaptive multi-band CFAR Detection of an optical pattern with unknown spectral distribution parameter. *IEEE Trans. Acoustics, Speech, and Signal Processing* 38, 1760-1770.
- Schwering P.B.W., van den Broek S.P., van Iersel M., (2007), in *Infrared Technology and Applications XXXIII*, eds. B.F. Andresen, SPIE Vol. 6542-100, 654230, Orlando Florida (USA), April 9-13, 2007: "EO System Concepts in the Littoral"
- Seijen, H.v., Schwering,P.B.W. & Bekman,H.H.P.T. (2004) *The Kvarn campaign NL-WP4 contribution band selection algorithms application to LWIR HBA(AHI) data*. JP8.10 document Th_T_WP4_K_01. 2004. TNO.
- Seijen, H.v., Schwering,P.B.W. & Bekman,H.H.P.T. (2005) *Hyper spectral Band Selection Algorithm*. Report FEL-04-A282. 2005. The Hague, TNO Physics and Electronics Laboratory.
- Toet, A. (2005) Colorizing single band intensified nightvision images. *Displays*, 26, 15-21. University of Delft, www.prtools.org
- Vagni, F. (2006) *Survey of Hyperspectral and Multispectral Imaging Technologies*. NATO Technical Report.
- Withagen P.J., den Breejen, E., et. al. (2001), "Band selection from a hyperspectral data-cube for a real-time multispectral 3CCD camera", *Proceedings of SPIE Vol. 4381*, pp 84-93
- Yamaguchi, Y., and R. J. P. Lyon, 1986, Identification of clay minerals by feature coding of nearinfrared spectra: in *Proceedings, International Symposium on Remote Sensing of Environment, Fifth Thematic Conference, "Remote Sensing for Exploration Geology"*, Reno, Nevada, 29 September- 2 October, 1986, Environmental Research.

APPENDIX: Presentations and performance results of Data set B.

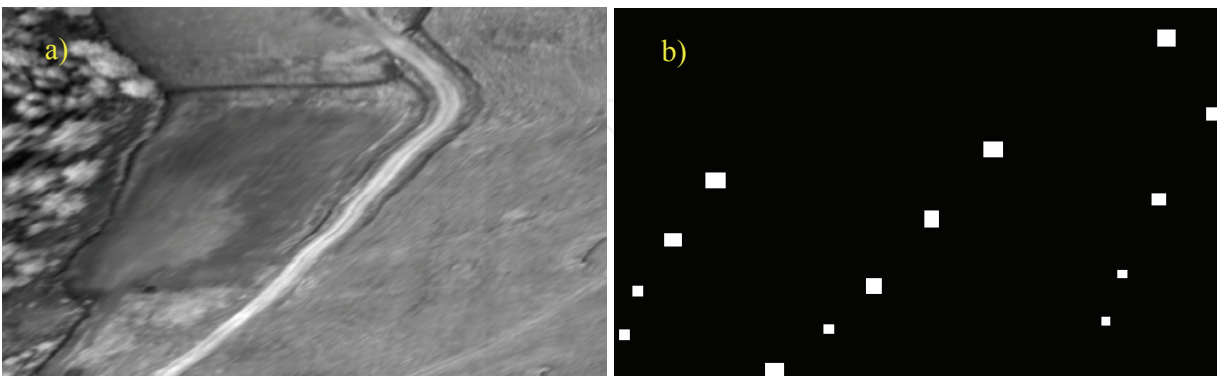


Fig. A1. Various presentation types of data set B, with a) the average, b) the designated target locations.

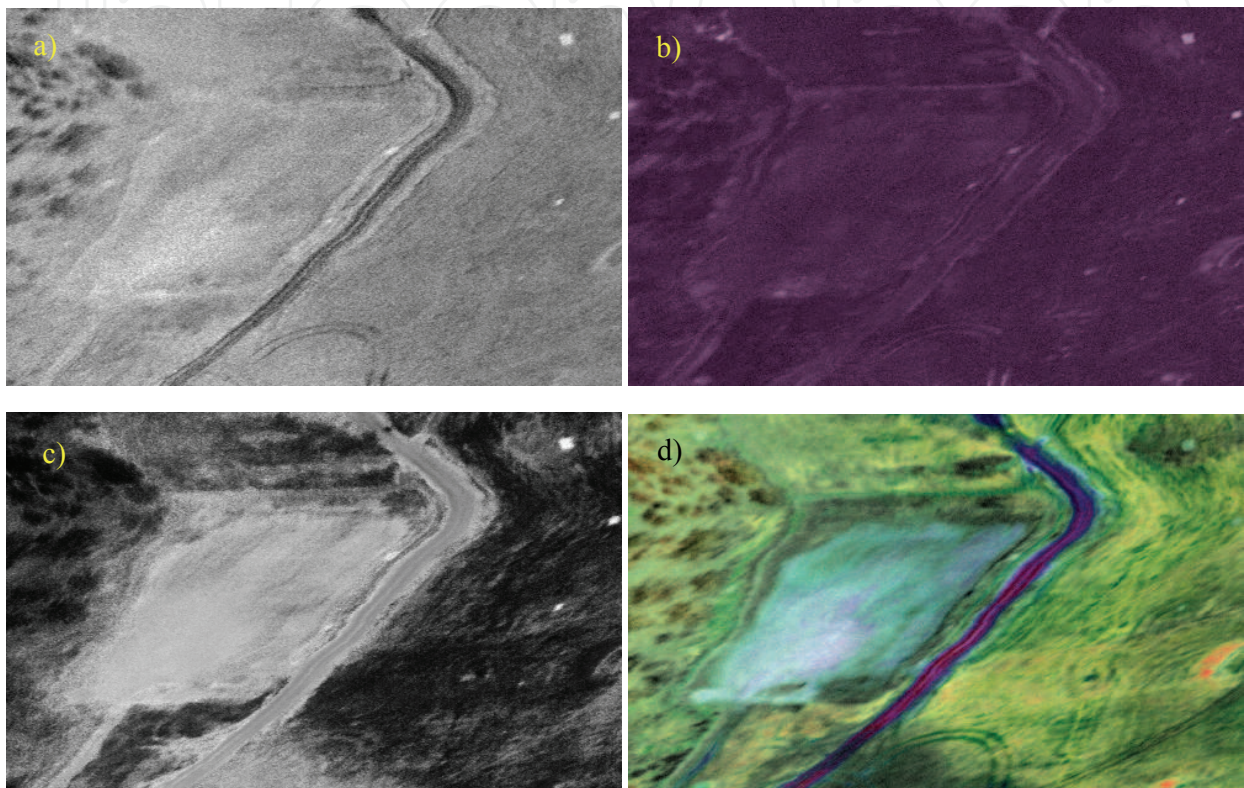


Fig. A2. Various presentation types of data set B, with a) band 37 of the movie sequence (the frame that reveals the targets best), b) anomaly, c) match with target 1 (highest target), and d) colour representation.

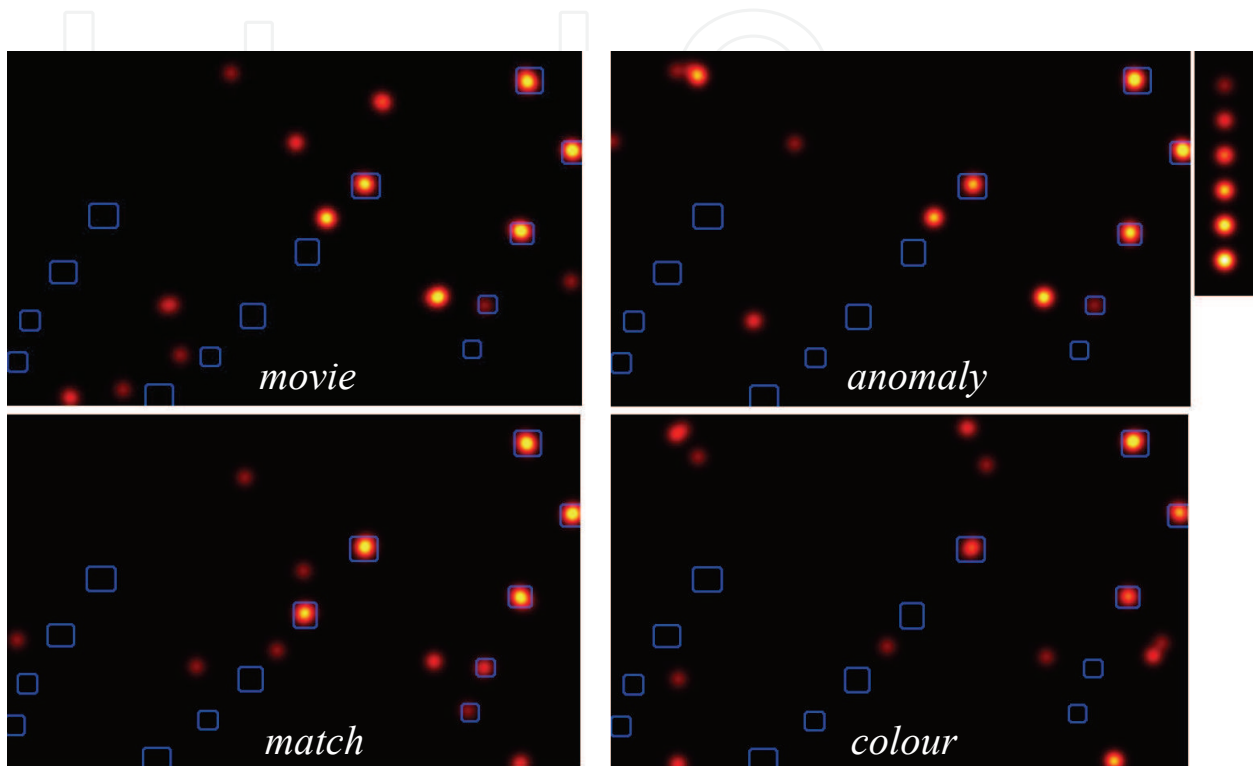
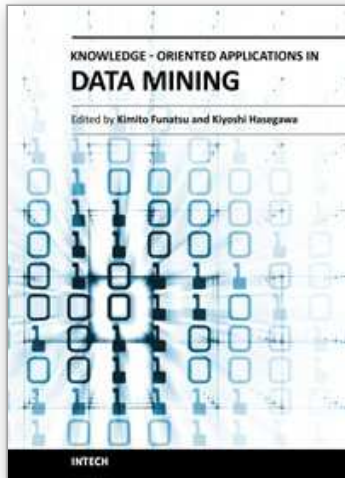


Fig. A3. Density graphs showing the density of target indications for the 4 different presentation types for data set B. The blue borders indicate the designated target positions.



Knowledge-Oriented Applications in Data Mining

Edited by Prof. Kimito Funatsu

ISBN 978-953-307-154-1

Hard cover, 442 pages

Publisher InTech

Published online 21, January, 2011

Published in print edition January, 2011

The progress of data mining technology and large public popularity establish a need for a comprehensive text on the subject. The series of books entitled by 'Data Mining' address the need by presenting in-depth description of novel mining algorithms and many useful applications. In addition to understanding each section deeply, the two books present useful hints and strategies to solving problems in the following chapters. The contributing authors have highlighted many future research directions that will foster multi-disciplinary collaborations and hence will lead to significant development in the field of data mining.

How to reference

In order to correctly reference this scholarly work, feel free to copy and paste the following:

Maarten A. Hogervorst and Piet B.W. Schwering (2011). Hyperspectral Data Analysis and Visualization, Knowledge-Oriented Applications in Data Mining, Prof. Kimito Funatsu (Ed.), ISBN: 978-953-307-154-1, InTech, Available from: <http://www.intechopen.com/books/knowledge-oriented-applications-in-data-mining/hyperspectral-data-analysis-and-visualization>

INTECH
open science | open minds

InTech Europe

University Campus STeP Ri
Slavka Krautzeka 83/A
51000 Rijeka, Croatia
Phone: +385 (51) 770 447
Fax: +385 (51) 686 166
www.intechopen.com

InTech China

Unit 405, Office Block, Hotel Equatorial Shanghai
No.65, Yan An Road (West), Shanghai, 200040, China
中国上海市延安西路65号上海国际贵都大饭店办公楼405单元
Phone: +86-21-62489820
Fax: +86-21-62489821

© 2011 The Author(s). Licensee IntechOpen. This chapter is distributed under the terms of the [Creative Commons Attribution-NonCommercial-ShareAlike-3.0 License](#), which permits use, distribution and reproduction for non-commercial purposes, provided the original is properly cited and derivative works building on this content are distributed under the same license.

IntechOpen

IntechOpen